

See discussions, stats, and author profiles for this publication at: <https://www.researchgate.net/publication/40884458>

# Average Orientation of Benzyl- d 5 Alkyl Ethers in Cationic Nematic Lyomesophases

ARTICLE *in* LANGMUIR · DECEMBER 1997

Impact Factor: 4.46 · DOI: 10.1021/la970560k · Source: OAI

---

CITATIONS

5

---

READS

25

3 AUTHORS, INCLUDING:



Ramiro Araya-Maturana

Universidad de Talca

92 PUBLICATIONS 475 CITATIONS

SEE PROFILE

# Average Orientation of Benzyl- $d_5$ Alkyl Ethers in Cationic Nematic Lyomesophases

Boris E. Weiss-López,<sup>\*,†</sup> Danilo Saldaño, Ramiro Araya-Maturana,<sup>‡</sup> and Consuelo Gamboa<sup>†</sup>

*Departamento de Química, Facultad de Ciencias, Universidad de Chile, Casilla 653, Santiago, Chile, and Departamento de Química Orgánica y Fisicoquímica, Facultad de Ciencias Químicas y Farmacéuticas, Universidad de Chile, Casilla 233, Santiago, Chile*

Deuterium quadrupole splittings from the aromatic ring of a series of linear benzyl- $d_5$  alkyl ethers, with alkyl chain length from 1 to 15 carbon atoms, have been measured using  $^2\text{H}$ -NMR spectroscopy. These molecules, 20% pentadeuteriated in the aromatic ring, were incorporated into type II cationic nematic lyotropic liquid crystals, made from tetradecyltrimethylammonium bromide (TDTMABr) and hexadecylpyridinium chloride (HDPyCl). Using these  $^2\text{H}$  quadrupole splittings, the two order parameters that completely describe the average orientation of the aromatic ring with respect to the direction of the magnetic field were estimated. Addition of these molecules did not have any appreciable effect on the integrity of either mesophase. An increase in the mobility of the  $Y$  molecular symmetry axis of the ring, on going from  $C_1$  to  $C_2$ , is observed in both mesophases. This observation suggests that the aromatic ring plane of benzyl methyl ether is oriented nearly parallel to the bilayer surface, although in HDPyCl it seems to be more mobile. As the alkyl chain length increases, progressive incorporation of the aromatic ring into the superstructure is observed. The opposite tendency of the quadrupole splitting of water between TDTMABr and HDPyCl is explained in terms of the location and orientation of the aromatic ring of the guest molecules and the symmetry and solvation capabilities of the head groups.

## Introduction

The location and average orientation of ions and molecules dissolved in solutions of aggregates made of surfactant molecules, as well as their mutual interactions, seem to depend on the properties of the guest species, the head group of the monomers that constitute the aggregate, the counterions, and the solvent. Furthermore, some of these host-guest interactions may have important consequences for the dynamics and structure of the aggregate.<sup>1-7</sup> NMR spectroscopy has been widely employed to obtain information about these systems.<sup>8-14</sup> The use of  $^2\text{H}$ -NMR quadrupole splittings is possibly one of the simplest methods to estimate molecular order parameters and, from these, to infer the average orientation, and sometimes the location, of guest molecules dissolved in anisotropic solutions. Recently, using  $^2\text{H}$ -NMR spectroscopy, we have measured the two order parameters that

completely describe the average orientation and have been able to infer the location of the aromatic ring in a series of linear  $N$ -alkylpyridinium- $d_5$  ions, dissolved in cationic and anionic nematic lyotropic liquid crystals.<sup>15,16</sup> All the mesophases studied by us were type II systems.<sup>17</sup> We found that addition of small amounts of pyridinium ions to liquid crystal solutions made from hexadecylpyridinium chloride (HDPyCl), tetradecyltrimethylammonium bromide (TDTMABr), and cesium decyl sulfate (CsDS) had an appreciable effect on the mobility of these interfaces. However, the integrity of the sodium decyl sulfate (SDS) interface was not significantly disturbed. These observations were rationalized in terms of the particular hydrophilic/hydrophobic properties of the alkylpyridinium ions and the solvation properties of the surfactant counterion. In all these situations the incorporation of the ions into the superstructure is with the  $C_2$  molecular symmetry axis of the aromatic ring nearly perpendicular to the bilayer surface. In this work, we have measured  $^2\text{H}$ -NMR quadrupole splittings to calculate the two order parameters that completely describe the orientation of the aromatic ring of a series of linear benzyl alkyl ethers, with alkyl chain length from 1 to 15 carbon atoms. These molecules, 20% pentadeuteriated in the aromatic ring, were dissolved in discotic lyotropic nematic liquid crystals (type II), made from TDTMABr and HDPyCl. Geometrical parameters of the guest molecules, necessary to calculate the order parameters from the observed quadrupole splittings, were obtained from fully optimized AM1 calculated structures.<sup>18</sup>

## Experimental Section

**Synthesis of Benzyl- $d_5$  Alkyl Ethers.** Benzyl- $d_5$  alkyl ethers were synthesized from a 20% v/v mixture of benzyl alcohol- $d_5$  (99%- $d_5$ ) and benzyl alcohol (P.A.). The sodium salt of this

<sup>†</sup> Departamento de Química.

<sup>‡</sup> Departamento de Química Orgánica y Fisicoquímica.

\* Abstract published in *Advance ACS Abstracts*, November 15, 1997.

(1) Heather, P.; Warr, G. G. *J. Phys. Chem.* **1996**, *100*, 16286.

(2) Palmer, B. J.; Liu, J. *Langmuir* **1996**, *12*, 6015.

(3) Mennucci, B.; Cossi, M.; Tomasi, J. *J. Phys. Chem.* **1996**, *100*, 1807.

(4) Hassan, P. A.; Valaulikar, B. S.; Manohar, C.; Kern, F.; Bourdieu, L.; Candau, S. J. *Langmuir* **1996**, *12*, 4350.

(5) Imae, T.; Kakitani, M.; Kato, M.; Furusaka, M. *J. Phys. Chem.* **1996**, *100*, 20051.

(6) Doisy, A.; Proust, J. E.; Ivanova, Tz.; Panaiotov, I.; Dubois, J. L. *Langmuir* **1996**, *12*, 6098.

(7) Quilliet, C.; Ponsinet, V.; Cabuil, V. *J. Phys. Chem.* **1994**, *98*, 3569.

(8) Radley, K.; McLay, N.; Lilly, G. J. *J. Phys. Chem.* **1996**, *100*, 12414.

(9) Casarotto, M. G.; Craik, D. J. *J. Colloid Interface Sci.* **1993**, *158*, 326.

(10) Seoud, O. A.; Blaskó, A.; Bunton, C. A. *Langmuir* **1994**, *10*, 653.

(11) Ylihautala, M.; Vaara, J.; Ingman, P.; Jokisaari, J.; Diehl, P. J. *Phys. Chem. B* **1997**, *101*, 32.

(12) Kimura, A.; Kuni, N.; Fuliwara, H. *J. Phys. Chem.* **1996**, *100*, 14056.

(13) Schmidt-Rohr, K.; Nanz, D.; Emsley, L.; Pines, A. *J. Phys. Chem.* **1994**, *98*, 6668.

(14) Veggeland, K.; Nilsson, S.; *Langmuir* **1995**, *11*, 1885.

(15) Weiss-López, B. E.; Gamboa, C.; Tracey, A. S. *Langmuir* **1995**, *11*, 4844.

(16) Weiss López, B. E.; Vicencio-González, J.; Gamboa C. *Langmuir* **1996**, *12*, 4324.

(17) Radley, K.; Reeves, L. W.; Tracey, A. S. *J. Phys. Chem.* **1976**, *80*, 174.

(18) Dewar, M. J. S.; Ziebis, E. G.; Healy, E. F.; Stewart, J. J. P. *J. Am. Chem. Soc.* **1985**, *107*, 3902.

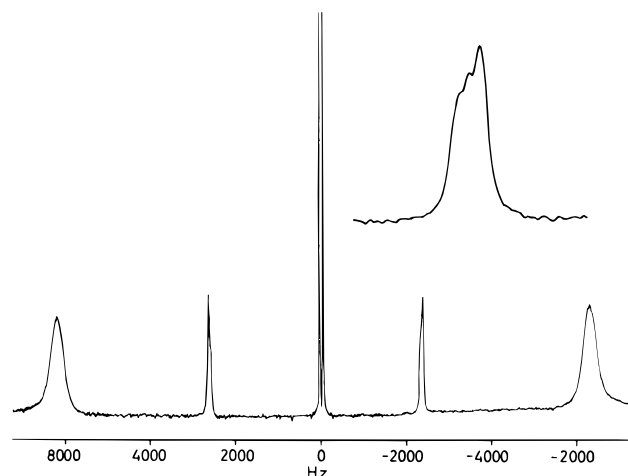


**Figure 1.** Deuterium NMR spectrum of benzyl- $d_5$  methyl ether, dissolved in HDPyCl mesophase. The central doublet arises from HDO, the outer doublet from decanol- $\alpha$ - $d_2$ , and the three internal doublets from positions ortho, meta, and para of the aromatic ring. The insert corresponds to expansion of the signal arising from the aromatic ring.

mixture was prepared by reaction with sodium hydride in anhydrous THF, under nitrogen. An excess of the respective alkyl halide, iodide for  $C_1$  and  $C_2$  and bromide for the others, was added to the solution and allowed to react for a period of 5 days at 298 K. The reaction was stopped by adding 5% aqueous HCl and thiosulfate. The product was separated from the reaction mixture by column chromatography, using silica gel as the stationary phase and chloroform as the eluent. The structures of the products were corroborated by  $^1\text{H}$ -NMR spectroscopy.

**Preparation of Mesophases.** The mesophases were prepared from commercially available TDTMABr and HDPyCl, previously recrystallized three times from ethyl acetate/ethanol mixtures and vacuum dried. TDTMABr samples were prepared by dissolving 0.21 g of TDTMABr, 0.1 g of NaBr, and 38  $\mu\text{L}$  of decanol (10%  $\alpha$ - $d_2$ ), in 0.5 mL of water (0.05%  $\text{D}_2\text{O}$ ). Between 4 and 6  $\mu\text{L}$  of ether, depending on the molecular weight of the ether, was added to this mixture. HDPyCl mesophases were prepared by dissolving 0.265 g of HDPyCl, 0.022 g of NaCl, and 60  $\mu\text{L}$  of decanol (10%  $\alpha$ - $d_2$ ), in 0.53 mL of water (0.05%  $\text{D}_2\text{O}$ ). The same amount of guest molecule was used for each sample in both mesophases.

**NMR Experiments.** All NMR spectra were recorded at 300 K on a Bruker AMX-300 NMR spectrometer at the Centro de Equipamiento Mayor (CEM), Facultad de Ciencias, Universidad de Chile. Deuterium NMR spectra were obtained using a broad band probe tuned to the deuterium frequency, and proton spectra were obtained using the proton channel of the same probe. A  $90^\circ$  flip angle (10  $\mu\text{s}$  pulse length), 32 kHz spectral window, 32 kB file size, and 30 transients/s were used for the deuterium spectra. Between 30 000 and 90 000 transients were accumulated to achieve a signal/noise ratio of 20.

## Results and Discussion

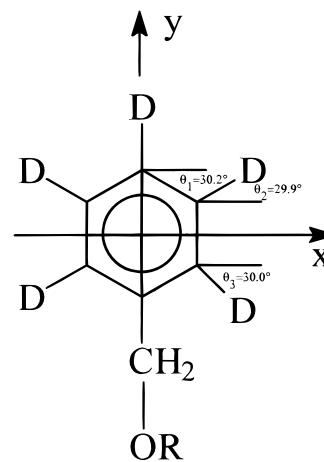
Figure 1 shows the  $^2\text{H}$ -NMR spectrum of benzyl- $d_5$  methyl ether dissolved in the type II magnetic field oriented nematic lyomesophase, prepared from HDPyCl. The insert corresponds to an expansion of the signals arising from the aromatic ring. The quadrupole splittings from DHO, decanol- $\alpha$ - $d_2$ , and positions ortho, meta, and para of the aromatic ring can be measured from the spectra. Table 1 summarizes all the experimental data of the present work, including the half-height width of the broad signal in the  $^1\text{H}$ -NMR spectrum of the dipole-coupled alkyl chains that constitute the aggregate,  $\Delta\nu_{1/2}$ . Figure 2 shows the structure of the studied molecules, along with the necessary geometrical information to calculate the order parameters.

Table 1 shows that in both mesophases the quadrupole splitting from decanol- $\alpha$ - $d_2$ , a measurement of the internal

**Table 1.** Deuterium Quadrupole Splittings from the Ortho, Meta, and Para Positions of the Aromatic Ring of Benzyl- $d_5$  Alkyl Ethers, from Decanol- $\alpha$ - $d_2$ , and from DHO in TDTMABr and HDPyCl Mesophases<sup>a</sup>

no. of carbons	DeOH- $\alpha$ - $d_2$	DHO	ortho	meta	para	$\Delta\nu_{1/2}$
TDTMABr Mesophase						
1	17 850	16	7682	7707	-6822	8180
2	18 399	15	8576	8576	-5225	8230
3	18 350	17	8796	8796	-5930	8250
4	18 430	17	9307	9307	-5980	8256
5	18 377	19	9587	9587	-6959	8300
6	18 360	19	9816	9816	-7567	8350
7	18 478	20	10177	10177	-7872	8170
8	18 295	19	10463	10463	-7950	8145
9	18 541	23	10938	10938	-7947	8270
10	18 471	23	11261	11261	-7840	8180
11	18 446	22	11542	11542	-7598	8193
12	18 670	23	12007	12007	-7497	8370
13	17 930	20	11850	11850	-7374	8050
14	18 180	20	12160	12160	-7890	8090
15	18 300	22	12370	12370	-7340	8080
HDPyCl Mesophase						
1	12 520	70	4976	5026	-4919	6200
2	13 636	72	6107	6107	-4097	6680
3	13 792	71	6416	6416	-4519	6580
4	13 743	68	6733	6733	-4282	6860
5	13 425	69	6660	6660	-4922	6480
6	13 475	67	6837	6837	-5397	6960
7	13 346	68	6913	6913	-5855	6550
8	14 006	69	7485	7485	-6387	6830
9	13 225	66	7290	7290	-6308	6744
10	13 442	67	7651	7651	-6460	6810
11	13 381	66	7896	7896	-6353	6660
12	13 846	67	8410	8410	-6478	6810
13	13 772	67	8651	8651	-6395	6650
14	14 040	68	9030	9030	-6392	6758
15	13 860	66	9025	9025	-6285	6860

<sup>a</sup> The half-height width of the dipole-broadened  $^1\text{H}$ -NMR spectrum is listed in the last column. The errors in the measured quadrupole splittings are  $\pm 1$  Hz for water,  $\pm 6$  Hz from  $C_1$  to  $C_6$  derivatives and  $\pm 20$  Hz for the others.



**Figure 2.** Structure of the studied molecules and designation of the molecular symmetry coordinates of the aromatic ring. The principal axis of the electric field gradient tensor is assumed to be in the direction of the C-D bond.

order of the interface, remains practically constant for all the samples: about 18 kHz in TDTMABr and 13 kHz in HDPyCl. This indicates that there is no appreciable effect of the added guest molecules on the integrity of the interface. Similar behavior is observed for the half-height width of the dipole-coupled broadened  $^1\text{H}$ -NMR signal from the oriented alkyl chains: it is practically constant for all the samples, about 8 kHz in TDTMABr and 6 kHz in HDPyCl. These two results show that there is no appreciable effect of the alkyl chain length of the added

guest molecules on the stability of the aggregate. Table 1 also shows the quadrupole splitting of HDO, a measure of the mobility of water molecules at the interface. In TDTMABr it has a value of about 16 Hz for the first members of the series, then increases to about 19 Hz for the intermediate size molecules, and increases again to about 21 Hz for the longer alkyl chain derivatives. The value of this parameter in the absence of added guest molecule is 21 Hz. This result indicates that the addition of the smallest derivatives modifies the ammonium head-group surface, increasing the mobility of water molecules close to it. Intermediate size derivatives have a similar effect but with less intensity, and the longer alkyl chain ethers do not seem to have any appreciable effect. Besides, the behavior of water at the HDPyCl interface is opposite to that observed in TDTMABr. In HDPyCl, the  $^2\text{H}$  quadrupole splitting of water increases from 61 Hz, in the absence of added guest molecules, to 70 Hz when benzyl methyl ether is incorporated. This effect experiences a small decrease when the alkyl chain length of the ether increases. As may be seen from Table 1, the quadrupole splitting of water in HDPyCl is always larger than that in TDTMABr, possibly as a consequence of the strong hydrophilic character of the pyridinium head group.<sup>15</sup> These observations will be discussed later in terms of the orientation of the aromatic ring on the surfaces, and the solvation properties of the different head groups.

Table 1 also shows the quadrupole splittings from the ortho, meta, and para positions of the pentadeuteriated aromatic ring. These benzyl alkyl ethers are more hydrophobic than the pyridinium analogs, and they should consequently be more strongly attached to the micelle. This is corroborated by the higher values of their quadrupole splittings, particularly for the shorter alkyl chain length derivatives. A closer inspection of Table 1 reveals that the quadrupole splittings from the ortho and meta positions were resolved only for benzyl methyl ether, in both mesophases. These splittings were not resolved for the other molecules of the series, possibly due to the increase in line width when mobility decreases, as a consequence of the longer alkyl chain length. The splittings from the ortho and meta positions, in both mesophases, increase along the series and trend to a constant value for the longer alkyl chain derivatives. The behavior of the quadrupole splitting from the para position is different. Unexpectedly, in both mesophases there is an increase of this value on going from  $\text{C}_1$  to  $\text{C}_2$ ; then it starts to decrease to finally trend to a constant value for the higher molecular weight derivatives.

To obtain detailed information about the average orientation of the aromatic ring of these benzyl alkyl ethers when incorporated into liquid crystal solutions of TDTMABr and HDPyCl, we have calculated the two order parameters that completely describe the average orientation of the aromatic ring,  $S_{xx}$  and  $S_{yy}$ , with respect to the direction of the magnetic field. For this purpose, we have used the experimental quadrupole splittings of the ortho and para positions and a previously reported equation<sup>19</sup> that relates these splittings with the order parameters, the deuterium quadrupole coupling constants ( $Q = 185$  kHz),<sup>20–22</sup> and the asymmetry parameter of the electric field gradient at the deuterium nucleus ( $\eta = 0.05$ ).<sup>20–22</sup> The exact values of these constants do not modify significantly the interpretation of our results. The neces-

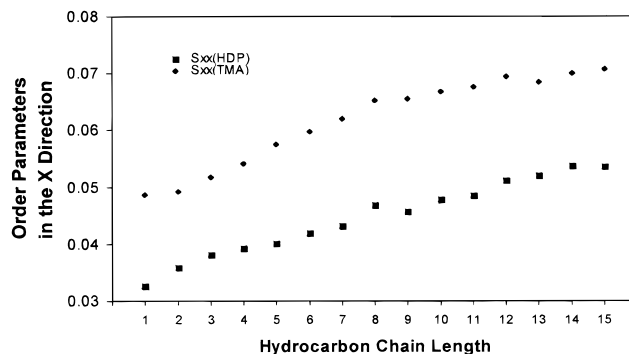


**Figure 3.** Order parameters along the  $X$  molecular axis of the aromatic ring of benzyl alkyl ethers in magnetic field oriented lyomesophases made from TDTMABr ( $\blacklozenge$ ) and HDPyCl ( $\blacksquare$ ), as a function of the alkyl chain length.

**Table 2.** Order Parameters,  $S_{xx}$  and  $S_{yy}$ , of the Benzyl Alkyl Ether Series, Dissolved in TDTMABr and HDPyCl Mesophases

no. of carbons	TDTMABr		HDPyCl	
	$S_{xx}$	$S_{yy}$	$S_{xx}$	$S_{yy}$
1	0.0487	-0.0350	0.0326	-0.0245
2	0.0493	-0.0303	0.0359	-0.0229
3	0.0518	-0.0331	0.0382	-0.0249
4	0.0542	-0.0340	0.0393	-0.0248
5	0.0575	-0.0379	0.0401	-0.0267
6	0.0598	-0.0405	0.0419	-0.0287
7	0.0620	-0.0421	0.0432	-0.0304
8	0.0635	-0.0427	0.0469	-0.0331
9	0.0656	-0.0433	0.0458	-0.0326
10	0.0668	-0.0433	0.0478	-0.0336
11	0.0676	-0.0428	0.0486	-0.0335
12	0.0695	-0.0430	0.0518	-0.0347
13	0.0685	-0.0424	0.0521	-0.0347
14	0.0712	-0.0430	0.0538	-0.0351
15	0.0708	-0.0429	0.0536	-0.0347

sary geometrical parameters for these calculations were obtained from full geometry optimization calculations, in the AM1 approximation. We performed these calculations for all the derivatives with the alkyl chain in the fully extended conformation. The geometry of the ring did not show any appreciable dependence on the alkyl chain length, and the optimized AM1 values were employed in the order parameters calculation. Figure 2 shows the designation of the molecular symmetry axis and the angle formed with the direction of the principal axes of the electric field gradient tensor at the deuterium nucleus, assumed to be along the C–D bond. Table 2 lists the calculated values of the order parameters,  $S_{xx}$  and  $S_{yy}$ , in both mesophases. An inspection of this table shows that the magnitudes of the calculated order parameters are greater for the TDTMABr mesophase. They are also bigger than the corresponding values of the pyridinium analogs, particularly the shorter alkyl chain length derivatives.<sup>15</sup> This is expected for more hydrophobic molecules. Figures 3 and 4 are plots of the calculated values of  $S_{xx}$  and  $S_{yy}$ , respectively, as a function of the alkyl chain length of the guest molecule, dissolved in HDPyCl and TDTMABr lyotropic nematic liquid crystals. As stated before,<sup>16</sup>  $S_{xx}$  mostly represents the motional average around the phenyl and benzylic methylene single C–C bond, essentially the internal coordinate that describes the torsional motion of the aromatic ring. Besides,  $S_{yy}$  mostly represents the motional average of the  $C_2$  symmetry axis of the ring. The order parameters can have values from  $-0.5$ , for an axis perpendicular to the magnetic field, to  $1.0$  for an axis parallel to the field, and  $0$  for a freely rotating axis or an axis oriented at the magic angle.

(19) Reeves, L. W.; Tracey, A. S.; Tracey, M. M. *Can. J. Chem.* **1979**, *57*, 747.

(20) Clymer, J. W.; Ragle, J. L. *J. Chem. Phys.* **1982**, *77*, 4366.

(21) Tsang, P.; Vold, R. R.; Vold, R. L. *J. Magn. Reson.* **1987**, *71*, 276.

(22) Catalano, D.; Forte, C.; Veracini, C. A. *J. Magn. Reson.* **1984**, *60*, 190.

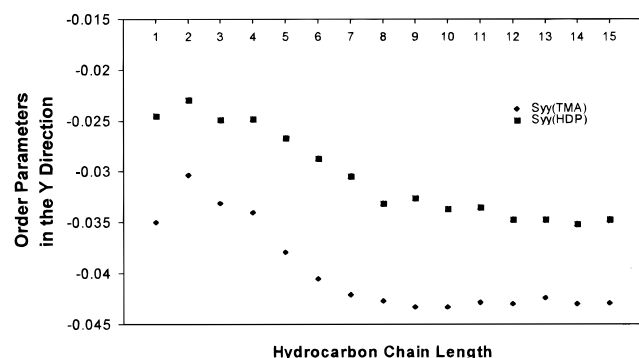


**Figure 4.** Order parameters along the  $Y$  molecular axis of the aromatic ring of benzyl alkyl ethers in magnetic field oriented lyomesophases made of TDTMABr (♦) and HDPyCl (■), as a function of the alkyl chain length.

In Figure 3 it may be seen that in TDTMABr  $S_{xx}$  remains practically constant for  $C_1$  and  $C_2$  derivatives and then increases to finally reach a constant value for the long alkyl chain length derivatives. At this point the ring of the guest molecule is totally incorporated into the surface. The profile of  $S_{xx}$  in HDPyCl is similar, except that in this mesophase  $S_{xx}$  always increases, even for the shortest alkyl chain length derivatives. As the alkyl chain length increases, the aromatic ring becomes more incorporated into the HDPyCl surface. A simple inspection of Figure 4 reveals that the behavior of  $S_{yy}$  is different. Unexpectedly, in both mesophases  $S_{yy}$  initially increases on going from  $C_1$  to  $C_2$ , and then it decreases to reach a constant value for the longer alkyl chain derivatives. At this point, the alkyl chain of the ether is completely incorporated into the superstructure of the aggregate. The observed initial increase of  $S_{yy}$  is indicative of an increase in the mobility of the  $Y$  molecular axis, and it is more pronounced in TDTMABr. An interpretation of these experimental observations may be suggested in terms of the following postulated model of incorporation of the guest molecules into the bilayer surfaces.

According to our model, in the TDTMABr mesophase the aromatic ring plane of benzyl methyl ether should be oriented nearly parallel to the surface formed by the ammonium head groups. A similar location for benzene rings has been proposed in order to explain the high contribution from the aromatic ring to the free energy of transfer of  $p$ -alkylphenols and phenoxides from water to spherical cetyltrimethylammonium bromide (CTABr) micelles. A specific interaction between the  $\pi$  electron cloud of the aromatic ring and the positively charged surface of the CTABr micelle has been suggested,<sup>23</sup> a possibility which has been mentioned several times before.<sup>24–28</sup> More recently, EPR spectra of some copper porphyrin derivatives incorporated into bilayers of dioctadecyldimethylammonium chloride<sup>29</sup> suggest that the long axis of the porphyrin is oriented nearly parallel to the ammonium surface. This evidence and our results seem to indicate that the orientation of the aromatic ring plane should be close to parallel to the bilayer surface. As the alkyl chain length of the ether increases, the hydrophobic effect becomes progressively more important, driving the alkyl chain more into the interior of the aggregate. This incorporation forces

the aromatic ring to become more perpendicularly oriented with regard to the bilayer surface plane. To achieve the new position, there must be a concomitant increase in the mobility of the  $Y$  axis of the ring. Furthermore, if the ring plane is initially very close to the bilayer surface plane, the mobility of the  $X$  axis, i.e., the torsional motion of the ring, should not be significantly affected by the increase in the mobility of the  $Y$  axis on going from  $C_1$  to  $C_2$ . These two behaviors of the order parameters  $S_{xx}$  and  $S_{yy}$  may be clearly observed in the TDTMABr mesophase (see Figures 3 and 4). Increasing the alkyl chain length of the ether induces the aromatic ring to become progressively more incorporated into the aggregate, and the mobility of both molecular axes decreases. The behavior of  $S_{yy}$  in HDPyCl is similar and suggests that in this mesophase a process equivalent to that observed in TDTMABr is occurring, except that the magnitude of the effect is smaller. This difference in magnitude may arise from a different orientation of the aromatic ring of the  $C_1$  derivative near the surface formed by the pyridinium head groups. We postulate that the plane of the aromatic ring of benzyl methyl ether is not as fixed, or as nearly parallel to the surface of HDPyCl, as it is in TDTMABr. Therefore, it does not need to increase its mobility as much as it does in the case of TDTMABr, to start to be incorporated into the HDPyCl surface structure.

The different behavior observed for the quadrupole splitting of water at these interfaces can be understood in terms of the orientation of the aromatic ring on the surfaces, discussed before, and the different symmetry and solvation properties of the head groups. The surface of ammonium head groups is very likely to be more hydrophobic than the surface of pyridinium head groups. A recent molecular dynamics simulation of  $n$ -decyltrimethylammonium chloride micelles in water, reveals that the interior of the micelle is significantly dry.<sup>30</sup> In general, pyridinium ions are very hygroscopic materials. Furthermore, the symmetry of the pyridinium head groups and the arrangement they have on the surface<sup>31</sup> may allow water molecules to be located more toward the interior of this head group than in the case of TDTMABr. A  $^1H$ -NMR study on the penetration of water in micelles showed that the alkyltrimethylammonium micelle interior seems to be drier than the cetylpyridinium micelle interior.<sup>32</sup> It also showed that protons at the ortho position of the pyridinium ring appear to be more hydrated than protons at the meta and para positions. The authors interpreted these results as a consequence of folding of the pyridinium head group back toward the aliphatic chain. Previous results on the pyridinium head group orientation in lyotropic liquid crystals of dodecylpyridinium iodide<sup>31</sup> and alkylpyridinium ions dissolved in cationic lyomesophases<sup>15</sup> indicate that the pyridinium moiety, when incorporated into the aggregate, is oriented toward the water-head-group interface. The fact that the ortho position of the pyridinium ring is more strongly solvated than the meta and para positions is a consequence of the strong hydrophilic character of the pyridinium moiety, attributable mainly to its high polarity and charge around the ortho position. These differences could explain the greater values observed for the quadrupole splitting of water in HDPyCl, and the different behavior observed for this parameter between both series of samples. The inclusion of the ether molecules, significantly hydrophobic substances, with their aromatic rings oriented nearly parallel

(23) Cabrera, J. W.; Sepúlveda L. *Langmuir* **1990**, *6*, 240.

(24) Bunton, C.; Sepúlveda, L. *J. Phys. Chem.* **1979**, *83*, 680.

(25) Hirose, C.; Sepúlveda, L. *J. Phys. Chem.* **1981**, *85*, 3689.

(26) Sepúlveda L.; Lissi, E.; Quina, F. H. *Adv. Colloid Interface Sci.* **1986**, *25*, 1.

(27) Mukerjee, P.; Cardinal, J. R. *J. Phys. Chem.* **1978**, *82*, 1620.

(28) Fendler, J. H.; Patterson, L. K. *J. Phys. Chem.* **1971**, *75*, 3907.

(29) Van Esch, J. H.; Feiters, M. C.; Peters, A. M.; Nolte, R. J. M. *J. Phys. Chem.* **1994**, *98*, 5541.

(30) Böcker, J.; Brickman, J.; Bopp, P. *J. Phys. Chem.* **1994**, *98*, 712.

(31) Tansho, M.; Ikeda, S.; Ohki, H.; Ikeda, R. *J. Phys. Chem.* **1995**, *99*, 4335.

(32) Bravo, C.; García-Río, L.; Leis, J. R.; Peña, M. E.; Iglesias, E.; *J. Colloid Interface Sci.* **1994**, *166*, 316.

to the TDTMABr bilayer surface, is very likely to increase the hydrophobic character of this surface, increasing the mobility of water located close to it. As the aromatic ring becomes more incorporated, and more perpendicularly oriented with regard to the bilayer surface, this effect becomes progressively smaller, to finally disappear for the high molecular weight derivatives, when the aromatic ring is significantly incorporated into the aggregate. This interpretation is consistent with the observed values of the quadrupole splitting of water throughout the series of samples in TDTMABr.

In HDPyCl the behavior of the quadrupole splitting of DHO is different: it initially increases for the shortest alkyl chain derivatives and then it experiences a small decrease along the series. The pyridinium head group is assumed to be hydrophilic. In a hexagonal phase, the pyridinium rings are probably stacked nearly parallel to each other, forming an angle of about  $45^\circ$  between the  $C_2$  symmetry axis of the ring and the ordering axis of the aggregate.<sup>31</sup> In this arrangement, it is very likely that water penetrates more deeply into the pyridinium head-group surface than into the ammonium surface. Therefore, the inclusion of the aromatic ring of the ether restricts the mobility of this incorporated water and decreases the exchange rate with the isotropic water molecules. Al-

ternatively, the water molecules should spend more time attached to the surface, increasing the quadrupole splitting.

Finally, in this work we have presented evidence that seems to indicate that, in the absence of significant hydrophobic interactions, the orientation of the aromatic ring plane of benzyl alkyl ether on the TDTMABr mesophase should be nearly parallel to the ammonium head-group surface, possibly due to a specific interaction between the aromatic  $\pi$  electron density and the positively charged ammonium surface. As the hydrophobic contribution increases, the orientation of the ring plane is progressively modified to finally become more nearly perpendicular to the bilayer surface. A similar process is observed in HDPyCl.

**Acknowledgment.** The authors are pleased to acknowledge financial assistance from Universidad de Chile, Grant D.I.D. Q3545-9633. We are also very pleased to thank Dr. Alan S. Tracey for invaluable suggestions and discussion. Finally, we want to thank Ms. Griselda Sagredo for technical assistance.